THE RFQ SECTION OF THE NEW UNILAC PRESTRIPPER ACCELERATOR AT GSI

U.Ratzinger, K.Kaspar, E.Malwitz, R.Tiede, GSI Darmstadt, Germany
S.Minaev, MEPI, Moscow, Russia

Abstract

The 1.4 MeV/u prestripper section of the UNILAC has to be rebuilt, to fill the Heavy Ion Synchrotron SIS up to its space charge limit. The injection and exit energies of the 36 MHz RFQ are 2.2 keV/u and 120 keV/u respectively. The design is made for I = 16.5 emA at a mass to charge ratio of 65. A new type of RFQ cavity for low rf frequencies which is operated in the H_{110}-mode was developed, the ´IH-RFQ´. The cavity is 9.25 m long and consists of 10 cylindrical modules with an inner diameter of 0.762 m. The shunt impedance will be around 600 kΩm.

1 INTRODUCTION

The design of heavy ion linacs is depending on the capability of available ion sources with respect to intensity, charge state, pulse lengths and transverse emittances. The generation of heavy ion beam pulses with a duration of typically 100 µs and intensities above 100 pµA is only possible at low ion charge states – up to 4+ above mass 180 – at present. The resulting high A/q values cause the need for new designs of key linac components – rf structures as well as focusing elements.

At GSI the 1.4 MeV/u Wideröe-section of UNILAC will be replaced by a new 36 MHz injector linac which accelerates ions as delivered from high intensity ion sources like CHORDIS and MEVVA [1].

It is planned to have a two beam time share operation at the new injector with up to 10 Hz/100 µs , 15 emA of U^{4+} MEVVA source and 50 Hz/5 ms, 200 eµA of U^{10+} PENNING source pulse trains.

This paper describes a new type of RFQ cavity which is especially well suited for operation below f ≅ 100 MHz. The cavity design, the rf and mechnical properties are reported.

The beam dynamics design and the PARMTEQ code simulations were done at the IAP-University Frankfurt [2]. MAFIA-studies about the rf field distribution are reported in ref. [3]. At present all components of the IH-RFQ are under construction.

2 RF MODE AND CAVITY DESIGN

The IH-RFQ has rf properties which are quite similar to the IH-DTL. Studies on IH-DTL´s to get the modes H_{111}, H_{110} or some intermediate field distribution – depending on the needs – were done at several laboratories [4].

In case of the RFQ structure the capacity per length and the electrode voltage along the cavity are kept constant. In that case the method of magnetic flux induction at the girder ends is used (fig. 2). The principle is corresponding to that of the vane undercuts used for 4 vane RFQ´s [5].

Compared to an IH-DTL at the same rf frequency the IH-RFQ inner tank diameter is by about a factor 2.2 smaller due to the increase of capacity per length by a factor 5. Compared to the 4 vane RFQ the IH-RFQ diameter again is smaller by about the same factor, due to the H_{110}-mode instead of the higher H_{210}-mode used for the 4 vane-RFQ (fig. 1). By allowing cavity diameters from 0.3 m up to 1.5 m, the IH-RFQ covers the important frequency range 18 MHz < f < 100 MHz for heavy ion acceleration. Another feature of the H_{110}-mode is the strong rf coupling along the cavity by the longitudinal magnetic field which allows to build long cavities with a stable voltage distribution.

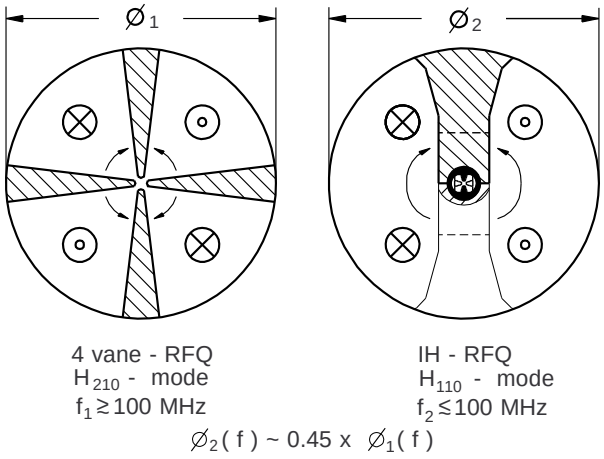

Fig. 1: Cross-sectional shape of the 4 Vane-RFQ and of the IH-RFQ with corresponding field orientations.

2.1 Mechanical Design

The design principle is explained by fig. 2, which shows the first and second module of the 36 MHz IH-RFQ. The complete cavity consists of 10 modules with identical lengths and diameters. The modular design enables the assembly of long tanks by bolting together cylindrical units of less than 1 m length.

The tank modules are made of carbon steel and will be copper plated electrolytically. The RFQ electrodes as well as their carrier rings are made from OFHC copper and will be brazed in the vacuum furnace.

The quadrupole electrodes are connected between modules by spring contacts which are located in the tank module flange planes. The alignment concept within one module relies on the precision of the central 100 mm bore along the beam axis where the carrier rings are accomodated. The technique used for that junction is similar to that applied at crankshaft bearings of combustion engines.

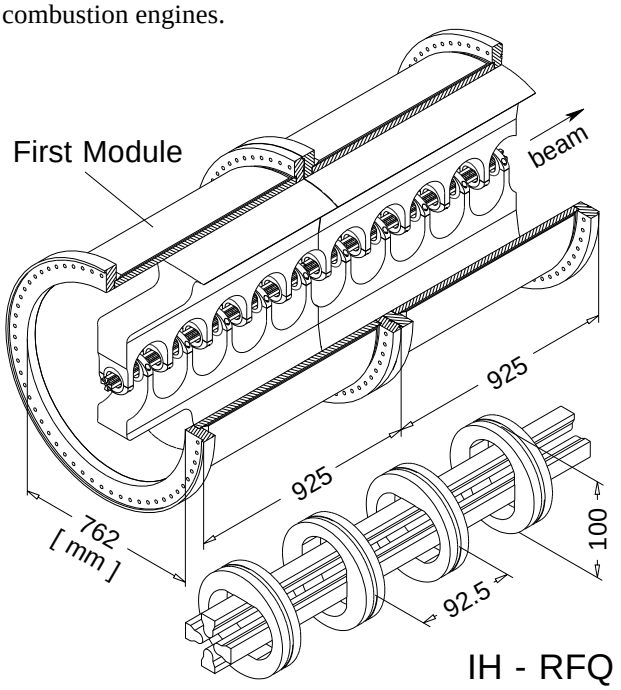

Fig. 2: First two modules of the IH-RFQ and enlarged illustration of the electrode structure with carrier rings.

2.2 Heat Losses, Thermal and Mechanical Stability

The homogeneous distribution of heat losses on the cavity surface due to the homogenous magnetic field distribution in the H_{110}-mode helps to reduce the efforts in water cooling. Typical numbers for the heat losses among components corresponding to the design as shown in fig. 2 are given in table 1 within the list of the main RFQ parameters.

Tabl. 1: List of the IH-RFQ parameters

injection energy / keV/u	2.2
exit energy / keV/u	120
total length / m	9.2
resonance frequency / MHz	36.136
inner diameter / m	0.762
shunt impedance / kΩm	~ 600
Q-value	~10000
electrode voltage / kV at A/q = 65	137
min. aperture diameter / mm	7.6
min. van-vane distance / mm	4.9
ρ/R_o	0.85
needed duty factors:	
for beams with A/q ≤ 65	1 %, 10 Hz
for beams with A/q ≤ 24	30 %, 50 Hz
distribution of heat losses / %:	
mini-vanes	4
stems with carrier rings	24
ridges	24
tank wall	48

The short distance of 92.5 mm between stem mid planes is essential to get the dipole content in the quadrupole field down to α ~0.002 and defining the potential of vertically opposed vanes as $V = V_0/2\cdot(1 \pm \alpha)$. The same distance parameter is also causing the low power losses on the mini vanes as discussed below.

2.3 Temperature Distribution along the Electrodes

A simplified model is used to calculate the temperature distribution along the mini vanes:

- the mini vane has a constant cross section
- the heat transport is calculated till to the mid plane of each stem along the electrodes without taking into account the stem thickness (this partly compensates for reduced heat conduction across the vane-stem junction)

The electric current along each mini vane is given by

$$I(z) = I_0 \cdot (1 - \frac{z}{z_0}); \qquad (1)$$

with $I_0 = K \cdot z_0$; $K = \frac{1}{2}\omega \cdot C' \cdot V_0$

$z = 0$: position at the middle plane of the contacted stem

$z = z_0$: position at the middle plane of the nearest neighbour stem, isolated against the electrode under consideration

V_0 = vane-vane voltage amplitude

C' = capacity per unit length of the 4 mini vanes.

If additionally an effective, reduced mini vane circumference b_{eff} corresponding to the electric power losses is defined, the temperature distribution along the electrode between two stems is given by:

$$T(z) = T_0 + \frac{\rho' \cdot K^2}{\lambda \cdot A \cdot b_{eff}} \cdot P(z); \qquad (2)$$

$$P(z) = \frac{z_0^3 z}{6} - \frac{z_0^2 z^2}{4} + \frac{z_0 z^3}{6} - \frac{z^4}{24}.$$

ρ' = surface resistance per unit area/Ω

λ = coefficient of thermal conductivity /W/(m·K)

A = averaged vane cross sectional area /m^2

b_{eff} = reduced vane circumference due to current distribution/m

Note the z_0^4-dependence of the temperature rise along the mini vanes!

The GSI-RFQ parameter choice results in an amplitude of the temperature oscillation along the mini-vanes of ΔT = 0.34 K at V_0 = 60 kV and a duty factor of 30 %. This allows a design with indirect water cooling of the mini vanes and their carrier rings only by heat conduction towards the water cooled stems.

The importance of short stem distances can additionally be seen by the formula describing the safety against buckling of a mini vane along the length 2 z_0 between two stems: The stability decreases proportionally to z_0^{-2} [6].

3 MINI VANE SHAPE AND MULTIPOLES

The beam dynamics calculations resulted in a design with a maximum electrode voltage of 137 kV at aperture radii in the range from 5.5 mm down to 3.8 mm [2]. From these numbers it becomes evident that the transverse cross section and especially the minimum distance between the electrodes is of great importance and has to be optimized with respect to three main goals:

- high break down voltage limit
- small multipole fractions additionally to the quadrupole field
- constant distribution of the electric capacity per unit length along the RFQ resulting in a flat voltage distribution.

As used in many RFQ designs before, the circular arc approximation with curvature ρ is taken for the vane tip geometry. Within each of the 10 modules an optimum ρ_i can be realized as the electrodes are fabricated separately for each module by use of a corresponding cylindrical cutter.

The first two goals of the optimization where treated by a small computer code based on the conventional field potential series [7] with the addition of an ´artificial´ boundary condition along the limiting curve of the investigated area: it has ellipsoidal shape and the voltage is changed between electrodes linearly along that path. By using that method the convergence of the potential series is extended from the RFQ aperture towards the outer electrode regions where sparking most probably occurs.

With respect to the third goal a first estimate was made by use of the semiempirical eq. (1) from ref. [8]. It was the starting point for detailed MAFIA-studies [3].

Finally PARMTEQ calculations including the 8-pole and 12-pole influence on the beam dynamics [2] and the encouraging test results from the 27 MHz RFQ prototype [9] as well as additional tuning methods with respect to the capacity distribution studies by the MAFIA-code resulted in a choice of ρ_i/R_i = 0.85 along the whole structure. 8- and 12-pole field strengths relatively to the quadrupole field at the minimum aperture radius of each module along the cavity are shown in Fig. 3.

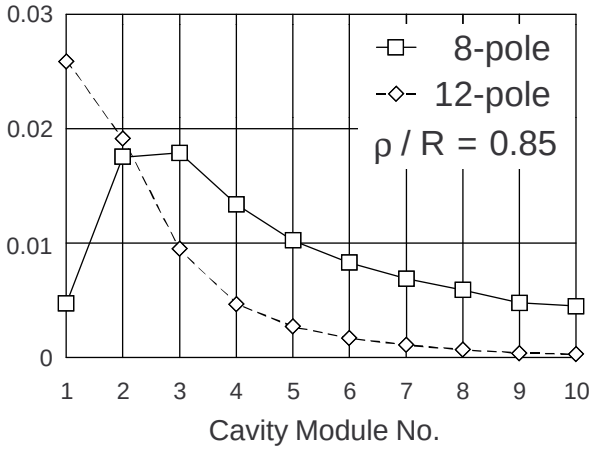

Fig. 3: 8-pole and 12-pole portions of the quadrupole strength normalized to the minimum aperture of each module.

ACKNOWLEDGEMENTS

We would like to thank K.M.Kleffner, MPI Heidelberg, for his kind support with MAFIA runs to check the dipole field contents in the IH-RFQ at the early design stage. The close and fruitful collaboration with A.Schempp, IAP Univ. Frankfurt is essential for the success of the project.

REFERENCES

[1] Beam Intensity Upgrade of the GSI Accelerator Facility, GSI-95-05 Report.

[2] A.Schempp, Particle Dynamics of the U^{4+} High Current RFQ, Int. Rep. S-95-10, IAP Uni Frankfurt.

[3] K.Kaspar, U.Ratzinger, Design of the GSI 36 MHz RFQ Section by MAFIA Calculations, these Proceedings.

4] U.Ratzinger, Interdigital RF Structures, Proc. of the 1990 LINAC Conf. Albuquerque, LA-12004-c, p. 525-529.

[5] M.J. Browman, G.Spalek and T.C.Barts, Studying the End Regions of RFQ´s using the MAFIA Codes, Proc. of the 1988 LINAC Conf., Williamsburg, CEBAF-Report-89-001, p. 64-66.

[6] Dubbel, Taschenbuch für den Maschinenbau, Springer-Verlag, 1987, Sect. C 7.1.

[7] I.M.Kapchinsky, Theory of Resonance Linear Accelerators, Harwood Academic Publishers, New York, 1985, Sect. 2.10.

[8] Ben-Zvi, A.Jain, H.Wong, A.Lombardi, Electrical Characteristics of a Short RFQ Resonator, as [4], p. 73-75.

[9] U.Bessler, A.Schempp, T.Sieber, J.Klabunde, P.Spädtke, Heavy-Ion-Beam and RF-Experiments with the 27 MHz Spiral-RFQ-Prototype, GSI-96-02 Report, p. 41.